Heliyon 10 (2024) e30107

Contents lists available at ScienceDirect

Heliyon

journal homepage: www.cell.com/heliyon

Research article

Landslide susceptibility assessment using deep learning considering unbalanced samples distribution

Deborah Simon Mwakapesa [a], Xiaoji Lan [a,*], Yimin Mao [b,c]

[a] School of Civil, and Surveying, & Mapping Engineering, Jiangxi University of Science and Technology, Ganzhou 341000, China
[b] School of Information Engineering, Jiangxi University of Science and Technology, Ganzhou 341000, China
[c] School of Information Engineering, Shaoguan University, Shaoguan 512005, China

ARTICLE INFO

Keywords:
Landslide susceptibility assessment
Deep learning
DNN
Unbalanced data
Loss functions

ABSTRACT

Landslide susceptibility assessment (LSA) is fundamental for managing landslide geological disasters. This study presents a deep learning approach (DNN-MSFM) designed to enhance LSA modeling, particularly addressing limitations caused by the unbalanced distribution of data samples in applied datasets. DNN-MSFM approach combines a deep neural network (DNN) and a mean squared false misclassification loss function (MSFM) to handle unbalanced samples from the algorithmic perspective. The model's performance was evaluated on an unbalanced dataset containing mapping units' records of 293 landslide samples and 653 non-landslide samples from the Baota District, China. Its effectiveness was assessed through statistical metrics and compared against DNN and Support Vector Machine (SVM) basic models. The results demonstrated a significant performance enhancement from the DNN-MSFM (OverallAccuracy = 0.889 and area under the receiver operating characteristic curve (AUC) = 0.84), indicating its effectiveness in learning the underlying landslide susceptibility features and demonstrating its ability to provide improved predictions even in areas with unbalanced landslide samples. Moreover, the study emphasizes the importance of considering balanced loss functions in training DNN under various imbalance degrees and contributes to expanding the applicability of DNN in LSA modeling. Also, this study builds a foundation for further enhancements of deep learning methods for geological disaster assessments.

1. Introduction

Landslides represent natural geological phenomena characterized by mass displacement of earth materials such as soil, debris, and rocks caused by various natural and human factors [1,2]. Landslide events not only cause direct damage to environmental facilities but also cause depletion of natural resources in the affected areas. Also, people residing in the landslide susceptible areas are the primary victims of landslides and experience massive fatalities of properties and even the lives of their dear ones [3,4]. Hence, managing and accessing landslide susceptible locations are essential in response to such damages and threats.

Landslide susceptibility assessment is an effective way to manage and assess landslides by predicting and demonstrating the probability and distribution of possible landslides in a certain area [5–7]. With the recent developments in computer technologies and the availability of data, several methodologies have been established to compute mathematical interactions between the landslide

* Corresponding author.
E-mail addresses: debrahmwaky@gmail.com (D.S. Mwakapesa), landcom8835@163.com (X. Lan), mymlyc@163.com (Y. Mao).

https://doi.org/10.1016/j.heliyon.2024.e30107
Received 23 January 2024; Received in revised form 18 April 2024; Accepted 19 April 2024
Available online 23 April 2024

factors and previous landslides to enhance landslide susceptibility assessment [8,9]. Generally, these methodologies can be characterized as knowledge-based and data-based methodologies [10–15]. Knowledge-based methodologies rely on geological knowledge and existing theories to assess landslide susceptibility in a certain region [11,16]. Provides a transparent and interpretable framework based on known principles, which can well-illustrate the underlying landslide mechanisms and deliver a clear and interpretable assessment framework. Nevertheless, due to its subjectivity, and the complex and dynamic nature of landslides, these approaches may not adjust well to dynamic environments. On the other hand, data-based methodologies primarily depend on data to assess and predict landslides and draw conclusions [17]. They exploit huge datasets to find the underlying patterns, and to their advantage, data-based approaches are more flexible to dynamic environments [14,15]. Deep learning models, a subcategory of machine learning, belong to the data-based methodologies that are progressively being employed to assess landslide susceptibility. This process employs multi-layered neural networks to systematically extract representations from data in a hierarchical manner [18–20].

The effectiveness of deep learning based LSA models relies significantly on both the algorithms employed, as well as the quality and quantity of data utilized [21]. Unlike other machine learning tasks, landslide susceptibility assessment usually has an unbalanced distribution of non-landslide (negative) and landslide (positive) locations (samples) in the datasets, a problem known as an unbalanced dataset [19,22]. This is because the non-landslide samples are widely available and can be selected randomly, while the ratio of landslide samples in the fields is usually low [23]. This problem can lead to unanticipated inaccuracies in the landslide susceptibility assessment models and even have severe consequences. This is due to the unbalanced distribution of samples, which pushes methods toward the non-landslide class, and the landslide features are not extracted effectively [24]. Hence, the basic methods (methods that do not consider an unbalanced dataset) are likely to misclassify the landslide samples into the non-landslide class, which can lead to relatively inaccurate landslide assessments [25,26].

In response to this, various methodologies have been pursued in the current literature. For example, some studies have recommended balancing the original dataset using sampling methods [27,28], data expansion using the SMOTE method [29], dice-cross entropy loss, and light gradient improving machine [30], and the use of semi-supervised learning to utilize the available non-landslide samples have been studies [22]. In other studies, the adaptive synthetic sampling method has been used to synthesize samples from the non-landslide areas by linear interpolation between the predominant samples in the non-landslide class [31]. However, most of these sampling approaches become ineffective for highly unbalanced datasets, and when sample distribution in the classes is unknown, the models may suffer from over-fitting or prompted bias problems and can cause loss of valuable information. Moreover, the unbalanced dataset problem has not been addressed well in the existing deep learning methods for modeling landslide susceptibility, as most of the current methods perform well on balanced datasets but may not guarantee accurate performance on unbalanced datasets.

Therefore, this study intends to address the limitation of the unbalanced distribution of samples in datasets used for deep learning-drive landslide susceptibility assessment from the algorithm perspective. Specifically, this study contributes an enhanced deep neural network (DNN-MSFM) that was developed based on a mean squared false misclassification (MSFM) loss function to explore DNN

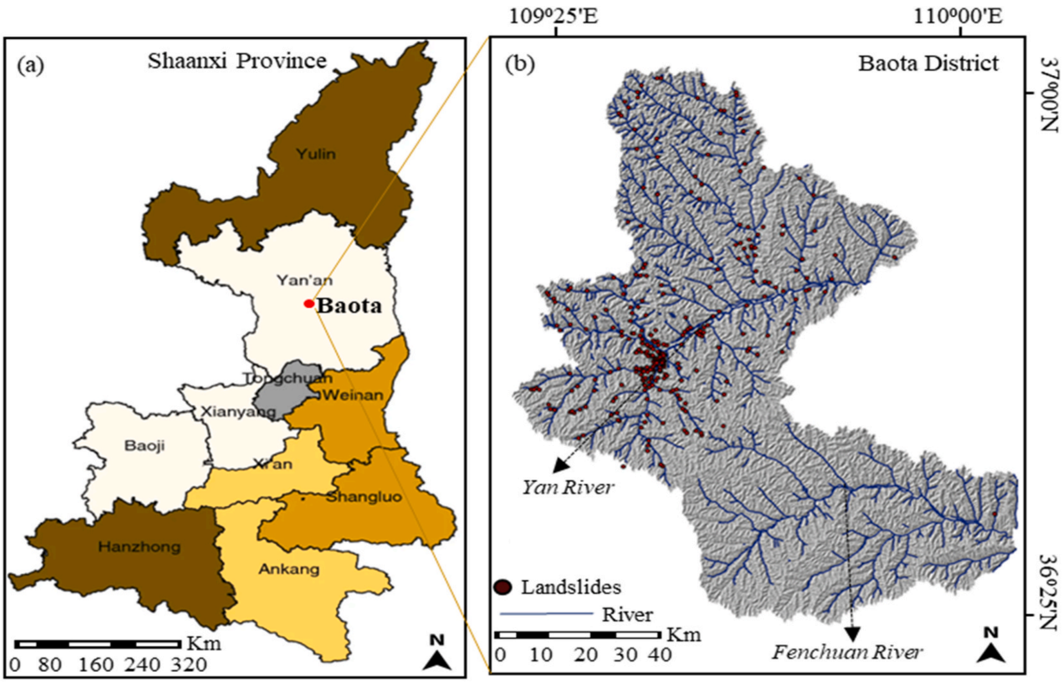

Fig. 1. Geographic location of the Baota district: (a) map of Shaanxi Province showing Baota district in the province; and (b) landslide inventory map portraying landslide distribution in Baota district.

performance and enhance its performance on the unbalanced dataset. This method makes the DNN training process sensitive to both non-landslide and landslide samples as well (the class of interest) and enhances a balanced performance for improved LSA. Also, this study demonstrates the significance of balanced loss function and shows how it could enhance the performance of DNN assessing landslide susceptibility. DNN-MSFM was experimented with using data from the Baota District, China, and 5 metrics were employed to measure the developed DNN-MSFM performance. The advantages and disadvantages of DNN-MSFM and its comparisons are also discussed.

Based on the current literature, this is the first time that the problem of unbalanced datasets has been addressed in DNN-based landslide susceptibility assessment specifically based on an algorithm perspective. This expands the applications of the highly beneficial DNN as it works well on both balanced and unbalanced datasets. In addition, the results will lay a solid basis for researchers and the relevant authorities to improve landslide management.

2. Materials

2.1. The study area

Baota is a 3556 km^2 district in Shaanxi Province, China (Fig. 1(a)). The area spans from a minimum altitude of 800 m to a maximum of 1400 m, while the latitudinal and longitudinal extents are 36° 11′N to 37° 02′N, and 109° 14′E to 110° 07′E, respectively. Baota experiences perennial average precipitation of about 500 mm–700 mm, mostly from June to August. The district is characterized by a mountainous and gravelly landscape [32–34]. There are three widely known mountains namely Fèng Huáng Shān (1165 m), Baota (1158 m), and Pagoda (1135 m). Yan and the Fenchuan Rivers flow in the northern and southern zones of the district, respectively, and approximately 60 % of the recorded landslides were observed along the Yan River [34,35]. The strata (Fig. 2) comprise Neogene red clay, Quaternary loess (which constituent about 80 % of the study area), as well as Jurassic and Triassic sandstone-mudstones. Also, the Loess Plateau (Huangtu Plateau) passes through the district characterizing it with thick and loose layers of loess sediments which make Baota very sensitive to various geological disasters. Frequent landslide disasters cause significant damage to the infrastructure and economic losses in the district, making them among the major obstructions to the expansion of various socioeconomic projects in this district [32,33]. Thus, the findings of this study are expected also to provide useful information for the assessment and management of landslide disasters.

2.2. Landslide inventory

The basis of landslide susceptibility assessment is that factors that caused historical landslides may define the likelihood of future landslide occurrence [2,38]. Hence, information about the geology, topography, and climate conditions of historical landslides in Baota was prepared to create a landslide inventory (Note: the information on sites and data on landslides were acquired from the collections of Xi'an Geological Survey Center). The collections included data extracted from aerial imageries, as well as QuickBird and SPOT 5 multispectral satellite imageries for the whole district and 225 km^2 of the township area, respectively. Fig. 1(b) depicts the

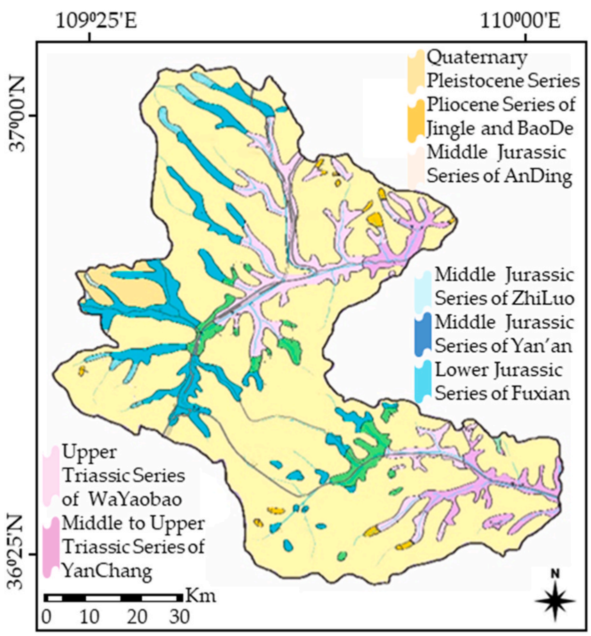

Fig. 2. The rock-soil strata in the study area [36,37].

created landslide inventory map. 1081 locations (samples) were investigated, out of which 293 locations had rainfall-induced landslide records [39,40], and 653 were non-landslide locations. It can be observed from Fig. 1(b) that most of the landslides were scattered along the Yan River tributaries. The landslide sizes scaled from small to large sizes with sliding volume ranging from less than $10^1 \times 10^4$ m^3 to $10^3 \times 10^4$ m^3 [36]. Thus, the dataset applied in this study contained 293 landslide and 653 non-landslide samples, indicating that, the ratio of landslide samples to non-landslide samples is approximately 0.448, and the landslide samples covers approximately 30.98 % only of the dataset. This demonstrates the unbalanced distribution in the dataset, with more non-landslide samples compared to landslide samples, which can significantly affect the model's performance, as addressed in this study.

2.3. *Landslide causative factors*

An essential and primary step in assessing landslide susceptibility is choosing a set of landslide-causative factors [41]. Based on the geological nature of Baota District, available data, as well as previous studies [42,43], 7 landslide causative factors were chosen in this study. Specifically, these factors included precipitation, altitude, aspect, curvature, vegetation (denoted by the normalized difference vegetation index (NDVI)), slope, and rock-soil structure (lithology).

The altitude, slope, curvature, and aspect were extracted based on Digital Elevation Model (DEM) at a resolution of 25 m. The literature has recorded that, the stability of altitude and slope ranged from 20 to 120 m and 25°–55°, respectively, and the shaded slopes were highly susceptible to landslides [44,45]. The geological data layer (strata, shown in Fig. 2) for rock-soil structure was determined by digitizing the study area geology map at 1:50,000 scale. The Vegetation layer was generated using remote sensing images captured by the Enhanced Thematic Mapper Plus sensors (ETM + RS images). Also, the precipitation indicates the instability of floppy rock-soil structure on a hill slope, thus, the average monthly precipitation data (recorded from 19 precipitation stations) was attained from the Weather Bureau of Baota [36,44], and the precipitation map was produced using the maximal mean monthly precipitation from July 2017 to 2018.

Moreover, it is commonly known that the classification method used for classifying the causative factors influences the predictive ability of a model [20,46–48]. The Jenks natural breakpoint/classification (JNC) process that is commonly used in LSA [49,50] was also applied here to classify the 7 factors as presented in Table 1 (illustrates the type, classification, and data sources for the landslide causative factors) [45]. The thematic layers of altitude, slope, aspect, curvature, NDVI, and precipitation factors were compiled and produced in ArcGIS Software (version 10.2), and are illustrated in Fig. 3(a–f).

2.4. *Data preparation*

Initially, the study area was rasterized to a raster map, and the whole area was distributed into 25 × 25 m 5,672,922 mapping units that were characterized by the 7 landslide-causative factors. The factor values were collected for each mapping unit. The mapping unit data for the investigated 293 landslides and 653 non-landslide locations) were randomly distributed into 70 % and 30 % for training and validating, respectively the model's performance. These procedures were facilitated by the ArcGIS 1.2 software. Moreover, as LSA is a binary classification task, during modeling, 0 is set to represent a non-landslide location while 1 represents a landslide location.

3. Methods

3.1. *Assessing the significance of landslide causative factors*

Selecting and assessing the most significant landslide causative factors are vital steps in LSA modeling [51,52]. For such purposes, the information gain ratio (IGR) method [22] is commonly employed. The IGR method quantifies the extent to which knowing the value of a specific factor contributes to the understanding of landslide susceptibility, thus, it helps to understand how much

Table 1
The factor's name, type classification, and data source.

Factor name	Factor type	Classification	Data source
Altitude	Continuous	<50, 50–60, 60–70, 70–80, 80–90, 100–110, 110–120, >120	Xi'an Geological Survey Center
Slope	Continuous	0–6.54, 6.54–13.08, 13.08–18.42, 18.42–22.78, 22.78–26.66, 26.66–30.54, 30.54–34.41, 34.41–39.02, 39.02–61.80	
Aspect	Discrete	Flat, N (North), NE (North-East), NW (North-West), E (East), W (West), SE (South-East), S (South), and SW (South-West)	
Precipitation	Uncertain	0~60, 60~80, 80~100, 100~120, 120 above	Baota Weather Bureau
NDVI	Continuous	< −0.477, −0.477 − −0.315, 0.314 − −0.193, −0.192 − −0.063, −0.062 − 0.073, 0.074 − 0.168, 0.169 − 0.237, 0.238 − 0.346, 0.347 − 0.495, >0.495	Xi'an Geological Survey Center
Curvature	Discrete	<-0.05, −0.05 to 0.05, >0.05	
Lithology	Discrete	1. Loess and almost flat paleosoil 2. Loess with sloped paleosoil 3. Loess, layers of paleosoil, and underlying bedrock 4. Loess, layers of paleosoil, and Neogene soil	

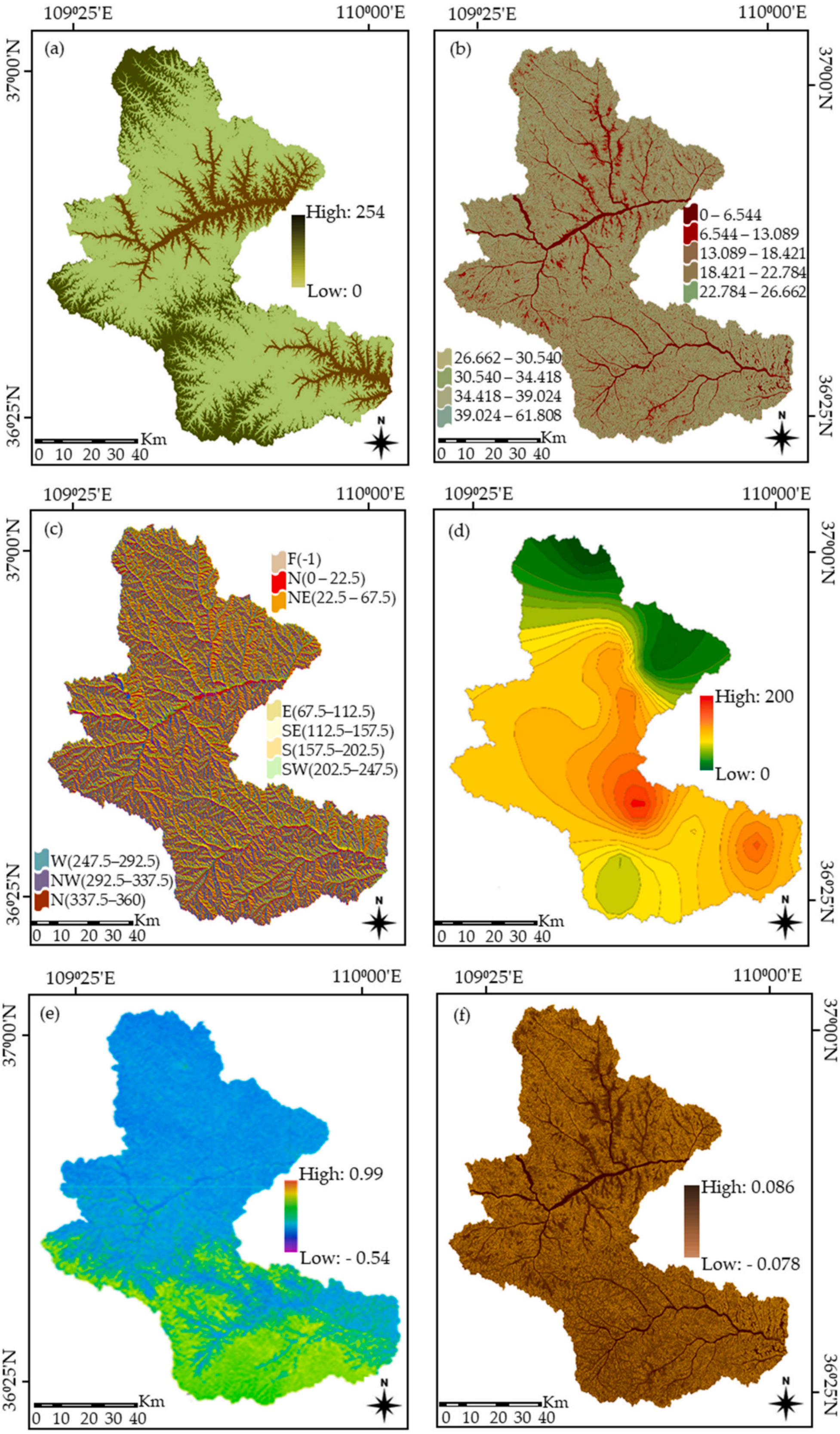

(caption on next page)

Fig. 3. Landslide causative factors (a) Altitude, (b) Slope, (c) Aspect, (d) Precipitation, (e) NDVI, (f) Curvature.

information about landslide susceptibility can be gained by considering such factors. Accordingly, IGR was employed to assess the significance of the 7 chosen factors to landslide susceptibility in the study area. This method is described as follows:

$$IGR(y / x_i) = E(y) - E(y / x_i) \quad (1)$$

$$E(y) = -\sum_{i=1}^{n} P(y_i) log_2(P(y_i)) \quad (2)$$

$$E(y / x_i) = -\sum_{i=1}^{n} P(y_i) \sum_{i=1}^{n} P(y_i / x_i) log_2(P(y_i)) \quad (3)$$

whereas, E is the entropy rate of the landslide causative factor x_i (with n classes = 2) equivalent to the predicted output y. $P(y_i)$ and $P(y_i / x_i)$ are the prior and posterior probabilities of y corresponding to x_i, respectively. IGR value ranges from 0 to 1, indicating least to most effective, respectively. Those causative factors that do not have much significance on landslide occurrence will have lower values (0) and can thus, be eliminated, while higher IGR values indicate higher factor significance in the occurrence of landslides and can be considered in LSA modeling [53].

3.2. The framework of the DNN-MSFM for landslide susceptibility assessment

As a classification task, landslide susceptibility assessment determines the likelihood of landslide susceptibility using available information [54]. However, since landslides do not happen everywhere, landslide samples in a certain area are usually few compared to the non-landslide samples; and as a result, the datasets are usually imbalanced and may cause significant errors. To address this, in this study, an improved DNN, DNN-MSFM framework was designed, and the classification of an unbalanced dataset was supported by collaborative learning. DNN-MSFM is constructed based on the structure of the basic DNN [20]. The framework is to understand the process that learns from an unbalanced dataset based on DNN-MSFM classification, aiming to alleviate the effect of the unbalanced dataset using an improved loss function and to enhance the performance [25,26,55]. The framework of the DNN-MSFM model is divided into three main parts: forward propagation, training with the modified loss function, and loss propagation (back-propagation). The framework is portrayed in Fig. 4, and explained below.

3.2.1. Forward propagation

DNN is a feature learning and classification technique that converts the raw data into advanced and theoretically accurate representations [56]. It comprises of an input layer, hidden layers, and one output layer [56]. DNN learns and extracts compound structures in huge datasets by alternating parameters, which are responsible for computing layers' representation consecutively [18,56]. Initially, the DNN model is trained during forward propagation, whereby, an unbalanced dataset described by a set of landslide causative factors is fed as inputs to the network through the input layer, and examined in the hidden layers. Lastly, the prediction class is shown in the output layer, and 2 likely outcomes (landslide and no landslide) can be predicted.

In the process, various parameters (for instance the quantity of hidden layers and neurons, along with the activation and transfer functions) are chosen initially to build the network for optimal performance. But, so far, there is no standard for setting such

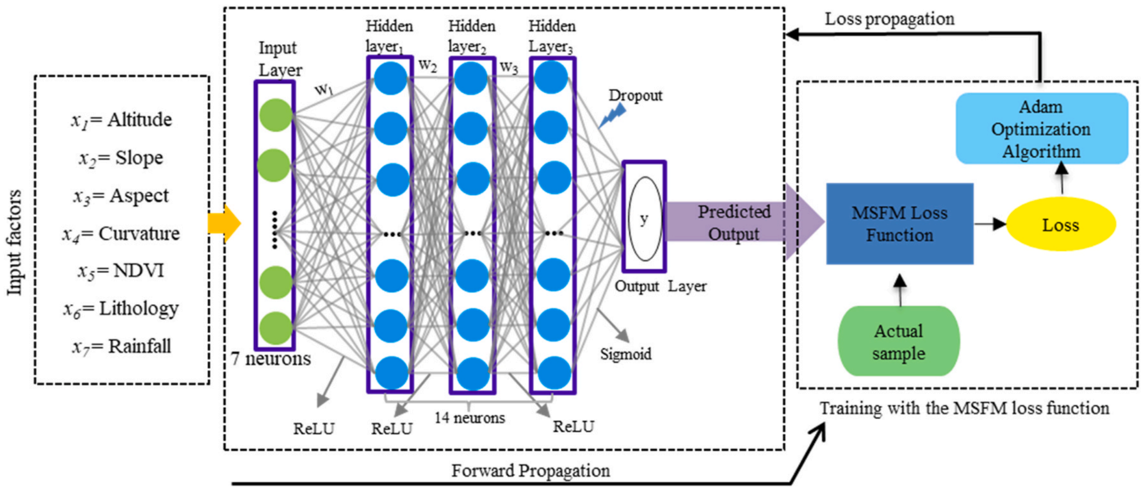

Fig. 4. The proposed framework of the DNN-MSFM used for assessing landslide susceptibility in the present study.

parameters. The neurons in the hidden layers consist of various weights (which are initially assigned randomly) and an activation function. Upon reaching the neuron, the inputs are weighted and added together to obtain the weighted sum, which is then given to the activation functions (including ReLU, Tanh, or Sigmoid) to generate the output [19,57]. These functions enhance the mapping of the inputs and outputs' non-linearity relation in the hidden layers.

3.2.2. *Training with the modified loss function*

The loss function is very important for DNN as it is used to regulate the network weights [58]. The output of the previous phase is compared with the true classes and the loss function computes a loss for any misclassification between the true classes and the output of the network which then evaluates the prediction performance of the network [59,60]. Small loss indicates high performance. The Mean Squared Error (MSE) function is normally used and was also used in the basic DNN [20], and it is expressed as in Eq. (4) below:

$$MSE = \frac{1}{T}\sum_{i}\sum_{j}\frac{1}{2}\left(a_j^i - y_j^i\right)^2 \tag{4}$$

where: T is the sum of all dataset samples, a_j^i and y_j^i are the actual and predicted outputs for the sample i on j neuron, respectively.

However, MSE is good for balanced datasets and doesn't work well with unbalanced datasets. This is because MSE detects the overall misclassification loss, i.e., the loss is calculated by first summing up all the squared misclassifications from the whole dataset and then finding their mean value. This can detect misclassifications from the non-landslide and landslide classes equally when the applied dataset is balanced. In the case of the unbalanced dataset, the misclassifications from the non-landslide class contribute more to the resultant loss than the misclassifications from the landslide class. This forces the MSE to be biased towards the non-landslide class and fails to detect the misclassifications from the two classes evenly. Consequently, DNN is more likely to learn and classify biased features from the non-landslide class, resulting in biased performance and misleading outcomes.

To overcome this limitation of the MSE loss function used in the basic DNN, the DNN-MSFM uses an improved MSE called mean squared false misclassification (MSFM) to enhance its performance for landslide susceptibility assessment. The false misclassification concept originates from false negative and false positive rates (FNR and FPR, respectively) derived from the error matrix [58,60], and are illustrated as follows:

$$FPR = \frac{1}{N}\sum_{i=1}^{N}\sum_{j}\frac{1}{2}\left(a_j^i - y_j^i\right)^2 \tag{5}$$

$$FNR = \frac{1}{P}\sum_{i=1}^{P}\sum_{j}\frac{1}{2}\left(a_j^i - y_j^i\right)^2 \tag{6}$$

whereby, FPR represents the false positive rate which detects misclassifications from the non-landslide class, and FPR represents the false negative rate which detects misclassifications from the landslide class. N and P signify the total numbers of samples in the non-landslide class, and landslide class, respectively.

Thus, MSFM can then detect the misclassifications both from the non-landslide class and landslide class equally by first calculating the average misclassification in each class, and then summing them together, as follows:

$$MSFM = \frac{1}{2}\left(FPR^2 + FNR^2\right) \tag{7}$$

$$= \frac{1}{2}\left((FPR + FNR)^2 + (FPR - FNR)^2\right) \tag{8}$$

By doing this, each class contributes to the ultimate loss value equally, and makes the loss sensitive to the misclassifications from both classes, in contrast to the MSE loss. Also, to obtain the minimum MSFM, DNN-MSFM minimizes $(FPR + FNR)^2$ and $(FPR - FNR)^2$ (misclassifications from both landslide and non-landslide classes) concurrently, which enhances DNN-MSFM to achieve balanced performance results in both classes, while maintaining high accuracy in the landslide class.

Table 2
Parameter setting of BDNN and DNN-MSFM.

Parameters	BDNN	DNN-MSFM
Number of hidden layers	3	3
Epochs	200	200
Learning rate	0.001	0.001
Activation function	ReLU	ReLU
Transfer function	Sigmoid	Sigmoid
Optimizer	Adam	Adam
Loss function	Mean squared error function	Mean squared false misclassification function

3.2.3. Loss propagation (back-propagation)

The information obtained from the MSFM loss function is transformed backward through the network, a process known as back-propagation [18,19]. The connection weights are then adjusted based on that information, and the process continues iteratively until the network can make correct predictions in most of the cases or until the lowest MSFM (as close to zero as possible) is obtained. By doing this, the model is optimized to the desired performance. In this study, the Adaptive moment optimization (Adam) [61] is used for back-propagation. Also, the dropout regularization technique (dropout = 0.5) is applied to avoid over-fitting and to enhance the generalization ability of DNN-MSFM.

It should be noted that, so far there are no guidelines on how to obtain the network parameters is still a topic of research in the DNNs training. In this study, several parameters were tried on the dataset, and the optimal parameters (such as ReLU activation, Sigmoid transfer function, Adam optimizer, 3 hidden layers, MSFM loss function, 200 epochs, and 0.001 default learning rate (Table 2)) made the network obtain the utmost performance were selected to build DNN-MSFM for LSA modeling. Finally, the prediction results generated by the constructed model can be rasterized in ArcGIS, and the outcomes are applied to create the susceptibility map.

3.3. Performance assessment

The performance assessment of the DNN-MSFM model was conducted to quantify its goodness of fit on the dataset and its predictive ability [2,38]. Thus, as the prediction of landslide susceptibility is structured as a binary classification, the values for true positive (TP), false positive (FP), true negative (TN), and false negative (FN) are estimated by assessing the actual and predicted values. Based on the results of these measures, the popular recall (sensitivity), OverallAccuracy, precision, F_Score and specificity [43,62–64], were calculated using Eqs. (9)–(13).

Also, the ROC curve was plotted using sensitivity against (1-Specificity) to examine the prediction rates and obtained the AUC values to evaluate the performance statistically [65]. The AUC values are ordered into 1 to 0.9, 0.9 to 0.8, 0.8 to 0.7, 0.7 to 0.6, and 0.6 to 0.5 indicating excellent, very good, good, and average performance [66–68].

$$Recall = \frac{TP}{TP + FN} \tag{9}$$

$$Specificity = \frac{TN}{FP + TN} \tag{10}$$

$$OverallAccuracy = \frac{TP + TN}{TP + TN + FP + FN} \tag{11}$$

$$Precision = \frac{TP}{TP + FP} \tag{12}$$

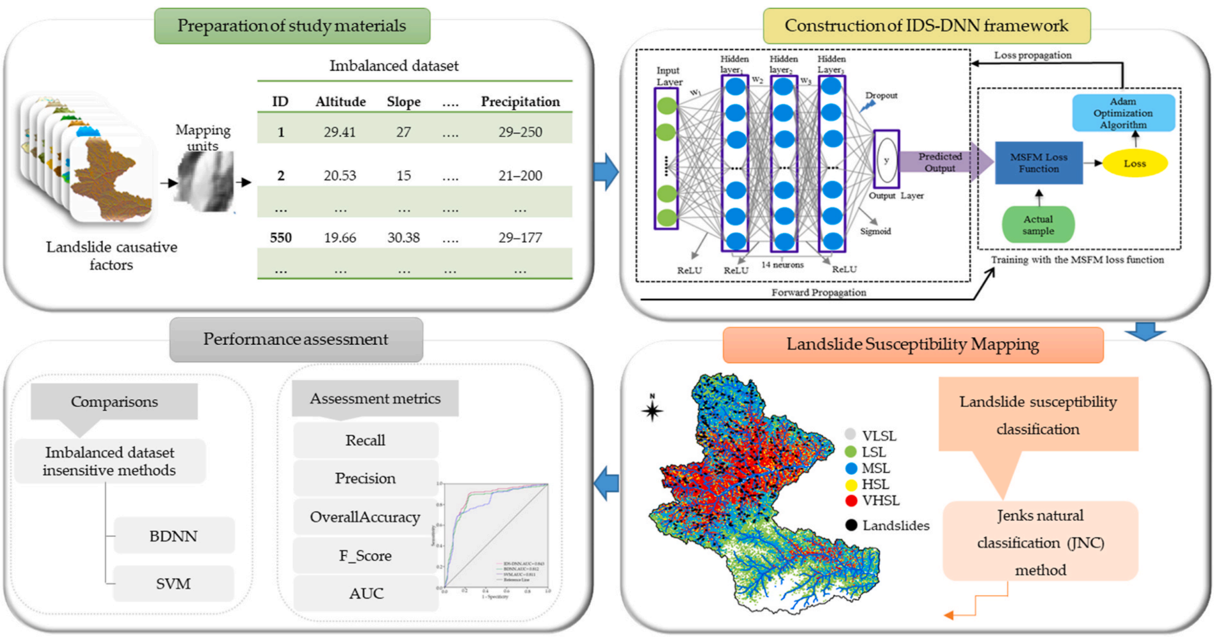

Fig. 5. The employed workflow for landslide susceptibility assessment.

$$F\_Score = 2 \times \frac{Precision \times Recall}{Precision + Recall} \quad (13)$$

Moreover, the performance results of the DNN-MSFM model were compared with unbalanced dataset-insensitive methods: the basic DNN (BDNN) and Support Vector Machine (SVM) models using the same dataset. BDNN illustrated in Ref. [20], was trained based on MSE loss function, and is used as the basic DNN for comparison in this study. Also, the SVM method which has been commonly used in constructing landslide susceptibility maps for different study areas in previous studies [69–72] was used for comparison. The comparison was carried out using the same metrics used for the performance assessment of the DNN-MSFM model described above.

3.4. Implementation framework

The proposed DNN-MSFM was employed in susceptibility mapping and its performance was assessed and compared with existing methods, in various steps as demonstrated in Fig. 5. To prepare data, the causative factor values were acquired from the thematic layers in ArcGIS, and subjected to the factors significance assessment. The resultant data we fed to DNN-MSFM for classification and prediction, whereby, following the framework described in Section 3, the method obtained one output (landslide or non-landslide) from the data. The obtained results were further categorized into 5 susceptibility classes using the JNC method, and then a susceptibility map was constructed. Then, various measures were applied to assess its results using a validation dataset and two unbalanced dataset-insensitive methods for comparisons.

4. Results

4.1. Results of the landslide causative factors significance assessment

The IGR method was employed to assess the significance of the designated factors and eliminate those factors with less or no influence on landslide susceptibility in the district. The assessment results are displayed in Table 3. When the information gain ratio value is higher and closer to 1, it indicates a higher significance of the selected causative factor in landslide event and was considered in modeling. Among them, precipitation had the uppermost influence on landslide (IGR value of 0.811), followed by lithology (0.783), altitude (0.657), slope (0.609), NDVI (0.548), curvature (0.436), and aspect (0.421). These results indicate that the 7 factors are effective for LSA modeling. Thus, none of the factors was eliminated and, they were all used in the subsequent modeling process.

4.2. Landslide susceptibility mapping

Following the DNN-MSFM framework described in Section 3.2, its prediction values were calculated in the ArcGIS software, and then based on the JNC method, the results were categorized into 5 landslide susceptibility levels/degrees: VLSL (very low), LSL (low), MSL (moderate), HSL (high), and VHSL (very high) [65]. The results were rasterized in ArcGIS and then applied to build the susceptibility map (Fig. 6), from which the percentages (%) of the land area covered by the landslide susceptibility degrees were estimated (Table 4).

4.3. Performance assessment and comparison results

Machine learning modeling comprises two stages: training and validation. In training, data from the training set are inputted into the model together with the expected output (true classes), and the model parameters are adjusted based on the model framework. In the validation stage, only the data from the validation dataset are inputted into the trained model to predict their outputs, which are then used to assess the model's performance. As described before, the dataset used for testing the DNN-MSFM model contained 30 % of the total dataset, which included 196 non-landslide samples and 128 landslide samples, reflecting the unbalanced state of the dataset.

Firstly, to assess and briefly demonstrate the classification and predictive performance of the DNN-MSFM on the unbalanced dataset, the samples in the dataset are distributed into three different imbalance degrees by reducing the representation of samples in one of the 2 classes to 15 %, 10 % and 5 % of samples, respectively. This means, for instance, that the 10 % imbalance degree means the samples in the landslide class equals 10 % of samples in the non-landslide class, and a smaller imbalance degree value indicates a more unbalanced dataset. This performance assessment was done in comparison to the BDNN model based on the OverallAccuracy and F_Score measures which are commonly used for performance assessment on unbalanced datasets. The assessment and comparison outcomes are shown in Table 5.

The results show that DNN-MSFM trained based on the MSFM loss function performed better than BDNN that was trained based on the MSE function on the same dataset with the corresponding imbalance degrees. For example at the imbalance degree of 15 %, the

Table 3
Feature selection analysis.

Factor	Precipitation	Lithology	Altitude	Slope	NDVI	Curvature	Aspect
IGR value	0.811	0.783	0.657	0.609	0.548	0.436	0.421

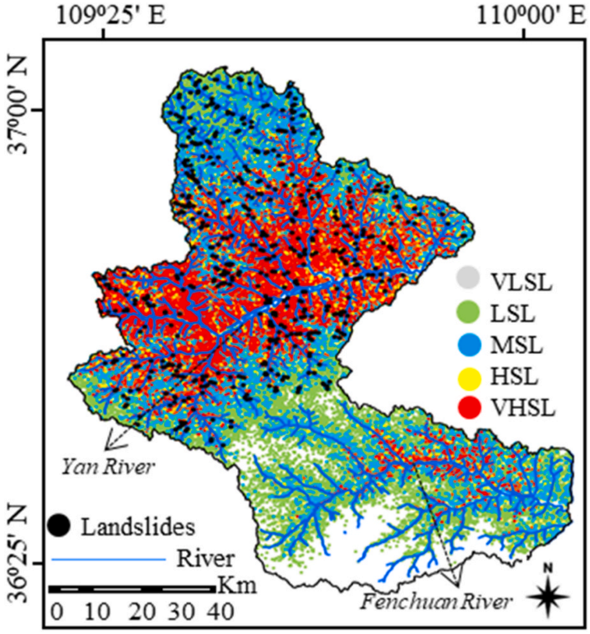

Fig. 6. Landslide susceptibility map constructed based on the DNN-MSFM.

Table 4
Description of the five landslide susceptibility degrees.

Degree of landslide susceptibility	Area coverage (%)
Very low (VLSL)	25.8
Low (LSL)	16.7
Moderate (MSL)	26.8
High (HSL)	14.7
Very high (VHSL)	16

From the map and the table, the distributions of the susceptibility degrees illustrated that the proportion of the moderate susceptibility degree was the highest, covering 26.8 % of the district, followed by very low (25.8 %), low (16.7 %), very high (16), and high susceptibility (14.7 %).

Table 5
Performance assessment under different imbalance degrees.

Imbalance Degree	OverallAccuracy		F_Score	
	BDNN	DNN-MSFM	BDNN	DNN-MSFM
15 %	0.813	0.819	0.515	0.59
10 %	0.795	0.800	0.408	0.471
5 %	0.696	0.798	0.191	0.295

DNN-MSFM obtained OverallAccuracy of 0.819 and F_Score of 0.59, while BDNN obtained OverallAccuracy of 0.813 and F_Score of 0.515. Also, as shown in the table, the DNN-MSFM model can improve its performance values more clearly when the dataset is highly unbalanced, indicating that the proposed model is also more effective when the dataset is highly unbalanced. This can be observed when the imbalance degree is 5 %, by replacing the MSE used in BDNN with MSFM in DNN-MSFM the OverallAccuracy and F_Score

Table 6
Performance of DNN-MSFM and compared methods (BDNN and SVM).

Model	Specificity	Accuracy	Recall	Precision	F_Score
DNN-MSFM	0.813	0.889	0.922	0.825	0.871
BDNN	0.842	0.830	0.813	0.722	0.765
SVM	0.786	0.775	0.758	0.698	0.727

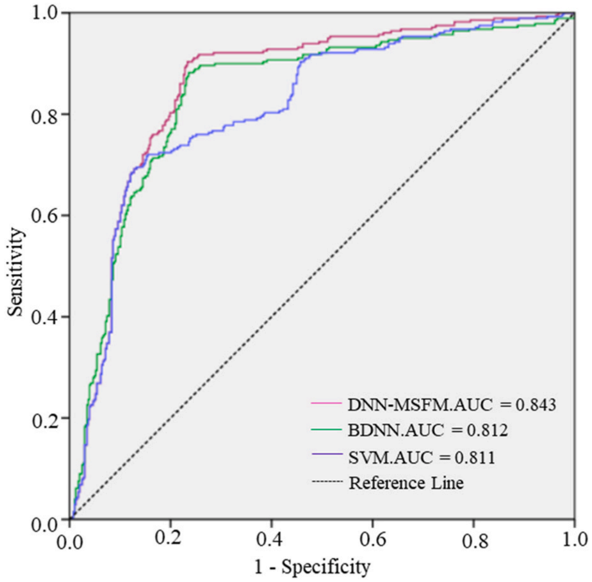

Fig. 7. ROC curves of DNN-MSFM and compared methods (BDNN and SVM).

values of DNN-MSFM were increased by 0.102 and 0.104 respectively, while the values increased by 0.06 and 0.075 only under the imbalance degree of 15 %. Generally, these results exhibit the efficacy of the DNN-MSFM framework described in this study over the existing BDNN on the unbalanced dataset.

Secondly, the DNN-MSFM's predictive performance results were tested using the whole test dataset (which is also originally unbalanced), and BDNN and the commonly used SVM were applied for comparison based on recall, OverallAccuracy, precision, and F_score statistical metrics (Table 6).

From the table, DNN-MSFM obtained the highest recall (0.922), and precision (0.825), followed by the BDNN model which obtained recall = 0.813, and precision = 0.722, while SVM obtained recall and precision values of 0.758 and 0.698, respectively. For correctly predicting both landslide and non-landslide samples, DNN-MSFM, BDNN, and SVM obtained OverallAccuracy values of 0.889, 0.830, and 0.775, respectively. Also, F_Score which is a good metric for the unbalanced dataset is used to compare models' performance by combining recall and precision values. Higher F_Score values indicate the better predictive competence of the model, and from the results DNN-MSFM, BDNN, and SVM obtained F_Score values of 0.871, 0.765, and 0.727, respectively, showing that among others, DNN-MSFM had the best predictive capability.

In addition to that, the models were compared using the ROC curves to find a model with optimal prediction with an AUC value as close to 1 as possible. The curves produced by the three models are displayed in Fig. 7, and the AUC values of DNN-MSFM, BDNN, and SVM are 0.8426, 0.8116, and 0.8109, respectively.

5. Discussion

LSA study is very effective for prevention and mitigation of landslides. Nowadays, deep learning models have gained much attention in landslide susceptibility assessment. However, the problem of an unbalanced dataset causes relatively unbalanced, poor, and unreliable performance of these methods, which then results in misleading conclusions from landslide susceptibility assessment studies. To address this problem, this study conducted a landslide susceptibility assessment using an improved deep neural network (DNN-MSFM) that was developed based on a mean squared false misclassification (MSFM) loss function. DNN-MSFM was implemented using data from the Baota District, China; and its performance was inspected using various metrics and compared with BDNN and SVM unbalanced dataset-insensitive models.

A landslide is a complex natural hazard associated with several causative factors that function together for its occurrence. During landslide susceptibility assessment, the selection and analysis of important factors have significant impacts on the assessment model's results. Yet, it is known that there is no typical method or rule for choosing factors. Seven factors were selected in this study to assess the Baota District's landslide susceptibility. The IGR technique was employed in this study to examine the importance of those factors in landslide susceptibility. The analysis results indicated that precipitation had the uppermost impact on landslide (IGR value of 0.811) which corresponds to previous studies conducted in the study area that also suggest that precipitation was the main cause of most landslides in the area (as since 1985, about 84 % of the recorded landslide events happened during the rainy seasons) [42,45,65]. Following this was the lithology, elevation, slope, NDVI, curvature, and aspect, signifying that those 7 factors are effective for LSA modeling. Thus, none of the factors was eliminated and, they were all used in the succeeding modeling procedures.

Since the goal of landslide susceptibility assessment models is to use the prevailing landslide data to depict the distribution of susceptible areas in the area, the generated susceptibility map reflects this goal successfully. The inventory map shown in Fig. 1(b) indicated that landslides are mostly scattered in the center to the northern peripheries of the district which are characterized by Quaternary loess, high precipitations, high elevated slope, shaded and west-facing slopes, as well as poor and scarce vegetation. The DNN-MSFM-based landslide susceptibility map demonstrated that most of the center, northeast, west, and northwest peripheries of the District are more susceptible to landslides at moderate to very high susceptibility, especially around the Yan River. The dissemination of very low and low landslide susceptibility was also observed in the southern part along the Fenchuan River and its tributaries, because of sufficient vegetation around the river basin that supports relatively stable slopes which are not easily susceptible to landslides. These assessments do not vary much with the inventory map and also comply with the study area characteristics from previous investigation records of the area.

DNN-MSFM performance assessment was done in different stages. Firstly, at different dataset unbalanced degrees, DNN-MSFM and compared BDNN performed poorly when the imbalance degree was higher, which was demonstrated by the overall decreasing trends of both OverallAccuracy and F_Score with increased imbalance degrees. However, in most cases, DNN-MSFM trained based on the MSFM loss function performed better than BDNN that was trained based on the MSE function with the corresponding imbalance degrees. It is also worth stating that the DNN-MSFM model could improve the OverallAccuracy and F_Score values more clearly when the dataset is highly unbalanced, indicating that the proposed model is also more effective when the dataset is highly unbalanced. This can also be observed when the imbalance degree is 5 %, by replacing the MSE used in BDNN with MSFM in DNN-MSFM the OverallAccuracy and F_Score values of DNN-MSFM were increased by 0.102 and 0.104 respectively, while the values increased by 0.06 and 0.075 only under the imbalance degree of 15 %. Generally, these results exhibit the efficacy of the DNN-MSFM framework described in this study over the existing BDNN on the unbalanced dataset. Also, with the MSFM loss function, DNN-MSFM guarantees better and more reliable performance compared to the BDNN model which uses an MSE loss function that is biased towards the non-landslide samples, which then causes biased performance results, hence, the reliability of BDNN performance results cannot be guaranteed.

Furthermore, the assessment of the predictive performance of DNN-MSFM was done using the whole test dataset, in comparison to BDNN and the commonly used SVM using recall, OverallAccuracy, precision, and F_score statistical metrics. The comparison results showed that DNN-MSFM obtained the highest recall (0.922), and precision (0.8252), implying that the DNN-MSFM has the best capability in distinguishing among the mapping units of landslide and non-landslide mapping units. Following this was the BDNN model which obtained recall = 0.813, and precision = 0.722, while SVM obtained recall and precision values of 0.758 and 0.698, respectively. For correctly predicting both landslide and non-landslide samples, DNN-MSFM, BDNN, and SVM obtained OverallAccuracy values of 0.889, 0.830, and 0.775, respectively. However, in some cases, OverallAccuracy can be a misleading metric when an unbalanced dataset is used, and it is usually not ideal to compare models with high recall values and low precision values, or vice versa, especially when the dataset is unbalanced. Thus, in this case, F_Score was used, and from the results DNN-MSFM, BDNN, and SVM obtained F_Score values of 0.871, 0.765, and 0.727, respectively, designating that among others, DNN-MSFM had the best predictive capability.

Not only that but also compared to other models, the AUC value of DNN-MSFM is very close to 1, indicating that it has the best performance. In general, with enhanced modified loss function (MSFM), DNN-MSFM obtained the best performance and appeared to be more effective when dealing with the unbalanced dataset than BDNN and SVM. Though the performance results of BDNN and SVM are somehow good, their reliability cannot be guaranteed. This is because; the two models are insensitive to the unbalanced dataset, and their performances are biased towards the non-landslide class rather than reflecting both landslide and non-landslide classes, which may result in misleading conclusions. If landslide assessment and mitigation measures root from such models, there will be a risk of misleading and incorrect conclusions, issues that can be successfully avoided by using the DNN-MSFM model with sufficient accuracy.

Generally, this study introduced several key innovations that significantly advance the LSA field. Firstly, the development of the DNN-MSFM approach addresses the critical issue of unbalanced datasets in LSA from an algorithmic perspective, enhancing the model's sensitivity to landslide samples and improving overall performance. Secondly, by integrating deep learning algorithms like DNN-MSFM, the study demonstrates a novel and effective LSA model, outperforming the unbalanced dataset-insensitive models in accuracy and reliability. Also, the study's emphasis on balanced loss functions and the importance of considering various imbalance degrees in training DNN models further contributes to expanding the utilization of deep learning application in LSA modeling.

While the current study presented a significant topic and satisfactory results, there are a few limitations associated with the study. The study selected seven factors only but mentioned the importance of the selected study area based on some human activities, and highlighted the frequency of landslide occurrence around the rivers, but factors such as land-use changes, human activities, and distance to the rivers that may influence landslide susceptibility were not accounted for in the assessment. Also, the underlying uncertainties associated with landslide susceptibility modeling, including training and validation datasets division methods, and trial setups of model parameters, can impact the reliability and robustness of the results.

6. Conclusions

This study presents a DNN-MSFM model for improved landslide susceptibility assessment, focusing on addressing the limitations of unbalanced datasets on DNN models, from an algorithmic perspective. DNN-MSFM was implemented using an unbalanced dataset from the Baota District, China; and a susceptibility map that reflects better the characteristics of landslide susceptibility in the district was constructed. The study's findings demonstrate the significance of using balanced loss functions and the importance of considering various imbalance degrees in training DNN models for improved landslide susceptibility assessment. The DNN-MSFM's success in addressing unbalanced datasets and providing higher performance with OverallAccuracy (0.889), AUC (0.843) and F_Score (0.871) compared to the unbalanced dataset-insensitive and existing models denotes its potential as a significant tool for landslide susceptibility assessment and management efforts.

Moreover, by considering the limitations of this study, further enhancements can be considered by integrating additional data sources to update the landslide inventory and exploring other geographical settings to examine the generalizability of DNN-MSFM. Additionally, by expanding the scope of the selected landslide causative factors, adopting more advanced modeling approaches and considering further experiments to evaluate the impact of using a balanced ratio on the susceptibility map the study can better capture the complex interactions behind landslide occurrence and improve the robustness of the susceptibility assessment, which can also be considered in further studies.

Funding statement

This research was supported by the National Natural Science Foundation of China (Grant No: 41561085).

Data availability statement

Data will be made available on request.

Additional information

No additional information is available for this paper.

CRediT authorship contribution statement

Deborah Simon Mwakapesa: Writing – review & editing, Writing – original draft, Visualization, Validation, Software, Resources, Methodology, Investigation, Formal analysis, Conceptualization. **Xiaoji Lan:** Writing – review & editing, Supervision, Resources, Project administration, Funding acquisition, Formal analysis. **Yimin Mao:** Writing – review & editing, Visualization, Validation, Supervision, Software, Resources, Project administration, Investigation, Data curation.

Declaration of competing interest

The authors declare no conflict of interest.

References

[1] W.-l. Xie, et al., Analysis of loess landslide mechanism and numerical simulation stabilization on the Loess Plateau in Central China, Nat. Hazards 106 (2021) 805–827.
[2] D. Asmare, Application and validation of AHP and FR methods for landslide susceptibility mapping around choke mountain, northwestern Ethiopia, Sci. Afr. 19 (2023) e01470.
[3] A.K. Turner, Social and environmental impacts of landslides, Innov. Infrastruct. Solutions 3 (2018) 1–25.
[4] S. Liu, et al., A comprehensive review of machine learning-based methods in landslide susceptibility mapping, Geol. J. 58 (6) (2023) 2283–2301.
[5] G. Duan, J. Zhang, S. Zhang, Assessment of landslide susceptibility based on multiresolution image segmentation and geological factor ratings, Int. J. Environ. Res. Publ. Health 17 (21) (2020) 7863.
[6] J. Gao, et al., Assessment of landslide susceptibility using different machine learning methods in Longnan city, China, Sustainability 14 (24) (2022) 16716.
[7] T. Zeng, et al., Tempo-spatial landslide susceptibility assessment from the perspective of human engineering activity, Rem. Sens. 15 (16) (2023) 4111.
[8] D. Ruidas, et al., Characterization of groundwater potential zones in water-scarce hardrock regions using data driven model, Environ. Earth Sci. 80 (2021) 1–18.
[9] P. Lima, et al., Literature review and bibliometric analysis on data-driven assessment of landslide susceptibility, J. Mt. Sci. 19 (6) (2022) 1670–1698.
[10] J. Roy, S. Saha, Landslide susceptibility mapping using knowledge driven statistical models in Darjeeling District, West Bengal, India, Geoenviron. Disasters 6 (1) (2019) 1–18.
[11] H. Kaur, et al., Knowledge-driven method: a tool for landslide susceptibility zonation (LSZ), Geol., Ecol., Landscapes 7 (1) (2023) 1–15.
[12] L. Yu, et al., Coupling data-and knowledge-driven methods for landslide susceptibility mapping in human-modified environments: a case study from Wanzhou County, three Gorges reservoir area, China, Rem. Sens. 14 (3) (2022) 774.
[13] A.-X. Zhu, et al., A similarity-based approach to sampling absence data for landslide susceptibility mapping using data-driven methods, Catena 183 (2019) 104188.
[14] L.D. Cengiz, M. Ercanoglu, A novel data-driven approach to pairwise comparisons in AHP using fuzzy relations and matrices for landslide susceptibility assessments, Environ. Earth Sci. 81 (7) (2022) 222.
[15] A.-X. Zhu, et al., A comparative study of an expert knowledge-based model and two data-driven models for landslide susceptibility mapping, Catena 166 (2018) 317–327.
[16] R. Senouci, et al., GIS-based expert knowledge for landslide susceptibility mapping (LSM): case of mostaganem coast district, west of Algeria, Sustainability 13 (2) (2021) 630.
[17] F. Huang, et al., Comparisons of heuristic, general statistical and machine learning models for landslide susceptibility prediction and mapping, Catena 191 (2020) 104580.
[18] K. Mandal, S. Saha, S. Mandal, Applying deep learning and benchmark machine learning algorithms for landslide susceptibility modelling in Rorachu river basin of Sikkim Himalaya, India, Geosci. Front. 12 (5) (2021) 101203.
[19] S. Xu, Y. Song, X. Hao, A comparative study of shallow machine learning models and deep learning models for landslide susceptibility assessment based on imbalanced data, Forests 13 (11) (2022) 1908.
[20] D.T. Bui, et al., Comparing the prediction performance of a Deep Learning Neural Network model with conventional machine learning models in landslide susceptibility assessment, Catena 188 (2020) 104426.
[21] F. Huang, et al., A deep learning algorithm using a fully connected sparse autoencoder neural network for landslide susceptibility prediction, Landslides 17 (2020) 217–229.

[22] J. Yao, et al., Assessment of landslide susceptibility combining deep learning with semi-supervised learning in Jiaohe County, Jilin Province, China, Appl. Sci. 10 (16) (2020) 5640.
[23] F. Huang, et al., Modelling landslide susceptibility prediction: a review and construction of semi-supervised imbalanced theory, Earth Sci. Rev. (2024) 104700.
[24] V. Vanto, M.I. Solihin, G. Sugiyanto, The effect of spatial scales and imbalanced data treatment on the landslide susceptibility mapping using Random Forest, in: AIP Conference Proceedings, AIP Publishing, 2023.
[25] C.X. Ling, V.S. Sheng, Cost-sensitive learning and the class imbalance problem, Encycl. Mach. Learn. 2011 (2008) 231–235.
[26] I. Cordón, et al., Imbalance: oversampling algorithms for imbalanced classification in R, Knowl. Base Syst. 161 (2018) 329–341.
[27] M. Ada, B.T. San, Comparison of machine-learning techniques for landslide susceptibility mapping using two-level random sampling (2LRS) in Alakir catchment area, Antalya, Turkey, Nat. Hazards 90 (1) (2018) 237–263.
[28] J. Dou, et al., Different sampling strategies for predicting landslide susceptibilities are deemed less consequential with deep learning, Sci. Total Environ. 720 (2020) 137320.
[29] W. Xueling, Y. Jingyu, N. Ruiqing, A landslide susceptibility evaluation method combining SMOTE and convolutional neural network, Geomat. Inf. Sci. Wuhan Univ. 45 (8) (2020) 1223–1232.
[30] S. Zhang, Y. Wang, G. Wu, Earthquake-induced landslide susceptibility assessment using a novel model based on gradient boosting machine learning and class balancing methods, Rem. Sens. 14 (23) (2022) 5945.
[31] D. Utomo, S.-F. Chen, P.-A. Hsiung, Landslide prediction with model switching, Appl. Sci. 9 (9) (2019) 1839.
[32] M.-s. Zhang, et al., A demonstration project for detailed geo-hazard survey in the Baota district, Yan'an, Northwest. Geol. 40 (2) (2007) 29–55.
[33] L. Guo, et al., GIS-based detection of land use transformation in the Loess Plateau: a case study in Baota District, Shaanxi Province, China, J. Geogr. Sci. 25 (12) (2015) 1467–1478.
[34] Y. Bai, et al., Land consolidation and eco-environmental sustainability in Loess Plateau: a study of Baota district, Shaanxi province, China, J. Geogr. Sci. 32 (9) (2022) 1724–1744.
[35] X. Qiang, Z. Maosheng, L. Lin, Loess landslide susceptibility evaluation based on slope unit and information value method in Baota District, Yan'an, Geol. Bull. China 34 (11) (2015) 2108–2115.
[36] M. Yimin, et al., Innovative landslide susceptibility mapping portrayed by CA-AQD and K-means clustering algorithms, Adv. Civil Eng. 2021 (2021).
[37] Y.-m. Mao, et al., Assessment of landslide susceptibility using DBSCAN-AHD and LD-EV methods, J. Mt. Sci. 19 (1) (2022) 184–197.
[38] C. Yu, J. Chen, Application of a GIS-based slope unit method for landslide susceptibility mapping in Helong City: comparative assessment of ICM, AHP, and RF model, Symmetry 12 (11) (2020) 1848.
[39] Y. Tang, et al., Field monitoring-based and theoretical analysis of Baota Mountain landslide stability, Adv. Civil Eng. 2021 (2021) 1–16.
[40] M.-s. Zhang, J. Liu, Controlling factors of loess landslides in western China, Environ. Earth Sci. 59 (8) (2010) 1671–1680.
[41] F. Huang, et al., Uncertainties of landslide susceptibility prediction: influences of random errors in landslide conditioning factors and errors reduction by low pass filter method, J. Rock Mech. Geotech. Eng. 16 (1) (2024) 213–230.
[42] Y. Mao, et al., Landslide susceptibility assessment using uncertain decision tree model in loess areas, Environ. Earth Sci. 76 (22) (2017) 1–15.
[43] D.S. Mwakapesa, et al., Landslide susceptibility mapping using DIvisive ANAlysis (DIANA) and RObust clustering using linKs (ROCK) algorithms, and comparison of their performance, Sustainability 15 (5) (2023) 4218.
[44] J. Hu, et al., A novel landslide susceptibility mapping portrayed by OA-HD and K-medoids clustering algorithms, Bull. Eng. Geol. Environ. 80 (2) (2021) 765–779.
[45] J. Hu, et al., Using uncertain DM-Chameleon clustering algorithm based on machine learning to predict landslide hazards, J. Robot. Mechatron. 31 (2) (2019) 329–338.
[46] Y. Tang, et al., Integrating principal component analysis with statistically-based models for analysis of causal factors and landslide susceptibility mapping: a comparative study from the loess plateau area in Shanxi (China), J. Clean. Prod. 277 (2020) 124159.
[47] F. Delgado, et al., Inventory of large landslides along the Central Western Andes (ca. 15°–20° S): landslide distribution patterns and insights on controlling factors, J. S. Am. Earth Sci. (2022) 103824.
[48] X. Luo, et al., Mine landslide susceptibility assessment using IVM, ANN and SVM models considering the contribution of affecting factors, PLoS One 14 (4) (2019) e0215134.
[49] P.T.T. Ngo, et al., Evaluation of deep learning algorithms for national scale landslide susceptibility mapping of Iran, Geosci. Front. 12 (2) (2021) 505–519.
[50] B. Pradhan, et al., A meta-learning approach of optimisation for spatial prediction of landslides, Rem. Sens. 13 (22) (2021) 4521.
[51] P.J. Jones, et al., Feature selection for unsupervised machine learning of accelerometer data physical activity clusters–A systematic review, Gait Posture 90 (2021) 120–128.
[52] D. Van Dao, et al., A spatially explicit deep learning neural network model for the prediction of landslide susceptibility, Catena 188 (2020) 104451.
[53] L. Zhu, et al., Landslide susceptibility prediction modeling based on remote sensing and a novel deep learning algorithm of a cascade-parallel recurrent neural network, Sensors 20 (6) (2020) 1576.
[54] A. Merghadi, B. Abderrahmane, D. Tien Bui, Landslide susceptibility assessment at Mila Basin (Algeria): a comparative assessment of prediction capability of advanced machine learning methods, ISPRS Int. J. Geo-Inf. 7 (7) (2018) 268.
[55] M.A. Febriantono, et al., Classification of multiclass imbalanced data using cost-sensitive decision tree C5. 0, IAES Int. J. Artif. Intell. 9 (1) (2020) 65.
[56] A.B. Adege, et al., Applying deep neural network (DNN) for robust indoor localization in multi-building environment, Appl. Sci. 8 (7) (2018) 1062.
[57] S. Saha, et al., Comparison between deep learning and tree-based machine learning approaches for landslide susceptibility mapping, Water 13 (19) (2021) 2664.
[58] P. Lyakhov, U. Lyakhova, D. Kalita, Multimodal Neural Network System for Skin Cancer Recognition with a Modified Cross-Entropy Loss Function, 2023.
[59] Q. Wang, et al., A comprehensive survey of loss functions in machine learning, Ann. Data Sci. (2020) 1–26.
[60] S. Jadon, A survey of loss functions for semantic segmentation, in: 2020 IEEE Conference on Computational Intelligence in Bioinformatics and Computational Biology (CIBCB), IEEE, 2020.
[61] D.P. Kingma, J. Ba, Adam: a method for stochastic optimization, preprint arXiv:1412.6980, arXiv (2014).
[62] Y. Mao, et al., Landslide susceptibility modelling based on AHC-OLID clustering algorithm, Adv. Space Res. 68 (1) (2021) 301–316.
[63] S. Nikoobakht, et al., Landslide susceptibility assessment by using convolutional neural network, Appl. Sci. 12 (12) (2022) 5992.
[64] D.M. Powers, Evaluation: from precision, recall and F-measure to ROC, informedness, markedness and correlation, preprint arXiv:2010.16061, arXiv (2020).
[65] D.S. Mwakapesa, et al., Landslide susceptibility mapping using O-CURE and PAM clustering algorithms, Front. Environ. Sci. (2023).
[66] C.X. Ling, J. Huang, H. Zhang, AUC: a statistically consistent and more discriminating measure than accuracy, Ijcai (2003).
[67] J. Huang, C.X. Ling, Using AUC and accuracy in evaluating learning algorithms, IEEE Trans. Knowl. Data Eng. 17 (3) (2005) 299–310.
[68] H. Bourenane, A.A. Meziani, D.A. Benamar, Application of GIS-based statistical modeling for landslide susceptibility mapping in the city of Azazga, Northern Algeria, Bull. Eng. Geol. Environ. 80 (10) (2021) 7333–7359.
[69] B.T. Pham, I. Prakash, Evaluation and comparison of LogitBoost Ensemble, Fisher's Linear Discriminant Analysis, logistic regression and support vector machines methods for landslide susceptibility mapping, Geocarto Int. 34 (3) (2019) 316–333.
[70] D. Xia, et al., Landslide susceptibility mapping based on the germinal center optimization algorithm and support vector classification, Rem. Sens. 14 (11) (2022) 2707.
[71] Q. Su, et al., Landslide Susceptibility Zoning Using C5, 0 decision tree, random forest, support vector machine and comparison of their performance in a coal mine area, Front. Earth Sci. (2021) 1181.
[72] S. Saha, et al., Novel ensemble of deep learning neural network and support vector machine for landslide susceptibility mapping in Tehri region, Garhwal Himalaya, Geocarto Int. 37 (27) (2022) 17018–17043.